Chapter 26B. Analysis of Imaging Spectrometer Data for the Takhar Area of Interest

By Raymond F. Kokaly and Michaela R. Johnson

Abstract

Imaging spectrometer data collected for the Takhar area of interest (AOI) in northeastern Afghanistan were analyzed with spectroscopic methods to identify the occurrence of selected materials at the surface. Absorption features in the spectra of HyMap data were compared to a reference library of spectra of known materials. Carbonates and muscovites cover most of the Takhar AOI. Distinct patterns of kaolinite clays and gypsum occur in localized patterns, especially in the center of the AOI. An analysis of HyMap data to detect gypsum was found to be effective in mapping the mineral in areas adjacent to the bedded gypsum deposit at Sary-Kan and the gypsum occurrence at Chal, and showing gypsum in coherent patterns stretching to the southwest and northeast of those known locations, spanning the entire AOI. Whereas halite does not have any strong diagnostic absorption features in the wavelengths covered by the HyMap imaging spectrometer, pixels that did not match any reference spectra and lack strong spectral features are distributed along the same trend as Chal-I and Chal-II salt deposits and the pixels in which gypsum was detected, indicating that these two map classes might be useful in refining our understanding of the distribution of this resource. The known coal deposits in the Takhar AOI appear to be associated with areas of kaolinite, kaolinite mixed with muscovite/clay/calcite, and calcite mixed with muscovite/illite classes.

26B.1 Introduction

Past studies of geologic data of Afghanistan revealed numerous areas with indications of potential mineral resources of various types (Peters and others, 2007; Abdullah and others, 1977). Several of these areas were selected for follow-on studies using imaging spectroscopy to characterize surface materials. Imaging spectroscopy is an advanced type of remote sensing also known as hyperspectral remote sensing. One area selected for follow-on study is the Takhar area of interest (AOI) in northeastern Afghanistan, which is approximately 230 km north of Kabul (fig. 26B–1). The area is believed to have the potential for coal, gypsum, and salt that are probably associated with Jurassic sedimentary rocks. To help assess these potential resources, high-resolution imaging spectrometer data were analyzed to detect the presence of selected minerals that may be indicative of past mineralization processes. This report contains the results of the spectroscopic data analyses and identifies numerous sites within the Takhar AOI that deserve further investigation, especially detailed geological mapping, lithologic sampling, and geochemical studies.

26B.2 Data Collection and Processing

In 2007, imaging spectrometer data were acquired over most of Afghanistan as part of the U.S. Geological Survey (USGS) project "Oil and Gas Resources Assessment of the Katawaz and Helmand Basins." These data were collected to characterize surface materials in support of assessments of resources (coal, water, minerals, and oil and gas) and earthquake hazards in the country (King and others, 2010). Imaging spectrometers measure the reflectance of visible and near-infrared light from the Earth's surface in many narrow channels, producing a reflectance spectrum for each image pixel. These reflectance spectra can be interpreted to identify absorption features that arise from specific chemical transitions and molecular bonds that provide compositional information about surface materials.

Imaging spectrometer data can only be used to characterize the upper surface materials and not subsurface composition or structure. However, subsurface processes can be indicated by the distribution of surface materials that can be detected using imaging spectroscopy data.

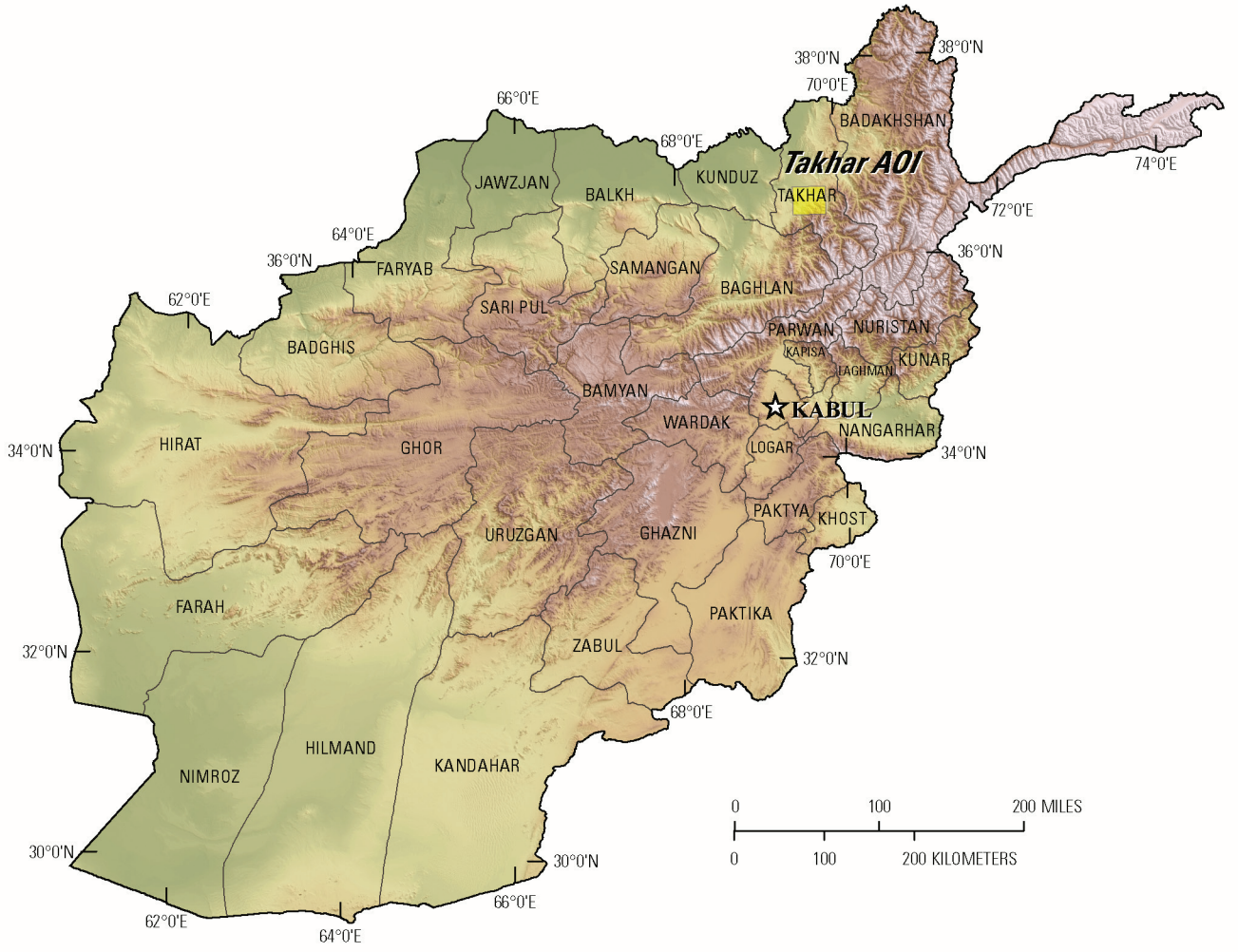

Figure 26B–1. Index map of the Takhar area of interest in northeast Afghanistan.

26B.2.1 Collection of Imaging Spectrometer Data

The HyMap imaging spectrometer (Cocks and others, 1998) was flown over Afghanistan from August 22 to October 2, 2007 (Kokaly and others, 2008). HyMap has 512 cross-track pixels and covers the wavelength range 0.43 to 2.48 microns (µm) in 128 channels. The imaging spectrometer was flown on a WB-57 high-altitude aircraft at 50,000 ft. There were 207 standard data flight lines and 11 cross-cutting calibration lines collected over Afghanistan for a total of 218 flight lines, covering a surface area of 438,012 km^2 (Kokaly and others, 2008). Data were received in scaled radiance form (calibrated to National Institute of Standards and Technology reference materials). Before processing, four channels that had low signal-to-noise ratios and (or) were in wavelength regions overlapped by adjacent detectors were removed from the HyMap data. Each flight line was georeferenced to Landsat base imagery in UTM projection (Davis, 2007).

26B.2.2 Calibration

HyMap data were converted from radiance to reflectance using a multistep process. This calibration process removed the influence of the solar irradiance function, atmospheric absorptions,and residual instrument artifacts, resulting in reflectance spectra that have spectral features that arise from the material composition of the surface. Because of the extreme topographic relief and restricted access to ground-calibration sites, modifications to the typical USGS calibration procedures were required to calibrate the 2007 Afghanistan HyMap dataset (Hoefen and others, 2010). In the first step of the calibration process, the radiance data were converted to apparent surface reflectance using the radiative transfer correction program Atmospheric CORrection Now (ACORN; ImSpec LLC, Palmdale, Calif.). ACORN was run multiple times for each flight line, using average elevations in 100-m increments, covering the range of minimum to maximum elevation within the flight line. A single atmospherically corrected image was assembled from these elevation-incremented ACORN results. This was done by determining the elevation of each HyMap pixel and selecting the atmospherically corrected pixel from the 100-m increment closest to that elevation.

Each assembled atmospherically corrected image was further empirically adjusted using ground-based reflectance measurements from a ground-calibration site. Five ground-calibration spectra were collected in Afghanistan: Kandahar Air Field, Bagram Air Base, and Mazar-e-Sharif Airport, as well as, soil samples from two fallow fields in Kabul. At each site, the average field spectrum of the ground target was used to calculate an empirical correction factor using the pixels of atmospherically corrected HyMap data in the flight lines that passed over the site. Subsequently, each of the HyMap flight lines was ground-calibrated using the empirical correction from the closest calibration.

To further improve data quality, an additional calibration step was taken to address the atmospheric differences caused, in part, by the large distances from calibration sites to acquired data. The large distances were a result of the lack of safe access to ground-calibration sites. The duration of the airborne survey and variation in time of day during which flight lines were acquired also resulted in differences in atmospheric conditions between standard flight lines and lines over ground-calibration sites, which were used to derive the empirical correction factors. Over the course of the data collection, the sun angle, atmospheric water vapor, and atmospheric scattering differed for each flight line. To compensate for this, cross-cutting calibration flight lines over the ground-calibration areas were acquired (Kokaly and others, 2008) and used to refine the reflectance calculation for standard data lines. A multiplier correction for standard data lines, typically oriented as north-south flight lines, was derived using the pixels of overlap with the well-calibrated cross-cutting lines, subject to slope, vegetation cover and other restrictions on pixel selection (Hoefen and others, 2010). As a result, the localized cross-calibration multiplier, derived from the overlap region, reduced residual atmospheric contamination in the imaging spectrometer data that may have been present after the ground-calibration step.

26B.2.3 Materials Maps and Presentation

After undergoing a complex and rigorous data calibration process, the georeferenced and calibrated reflectance data were processed. The reflectance spectrum of each pixel of HyMap data was compared to the spectral features of reference entries in a spectral library of minerals, vegetation, water, and other materials (King, Kokaly, and others, 2011; Kokaly and others, 2011). The best spectral matches were determined for each pixel and the results were clustered into classes of materials discussed below.

HyMap reflectance data were processed using MICA (Material Identification and Characterization Algorithm), a module of the USGS PRISM (Processing Routines in Interactive Data Language for Spectroscopic Measurements) software (Kokaly, 2011). The MICA analysis compared the reflectance spectrum of each pixel of HyMap data to entries in a reference spectral library of minerals, vegetation, water, and other materials. The HyMap data were compared to 97 reference spectra of

well-characterized mineral and material standards. The resulting maps of material distribution, resampled to 23 × 23 m square pixel grid, were mosaicked to create thematic maps of surface mineral occurrences over the full dataset covering Afghanistan.

MICA was applied to HyMap data twice to present the distribution of two categories of minerals that are naturally separated in the wavelength regions of their primary absorption features. MICA was applied using the subset of minerals with absorption features in the visible and near-infrared wavelength region, producing a 1-µm map of iron-bearing minerals and other materials (King, Kokaly, and others, 2011), and again using the subset of minerals with absorption features in the shortwave infrared, producing a 2-µm map of carbonates, phyllosilicates, sulfates, altered minerals, and other materials. For clarity of presentation, some individual classes in these two maps were bundled by combining selected mineral types (for example, all montmorillonites or all kaolinites) and representing them with the same color in order to reduce the number of mineral classes. The iron-bearing-minerals map has 28 classes. Iron-bearing minerals with different mineral compositions but similar broad spectral features are difficult to classify as specific mineral species. Thus, generic spectral classes, including several minerals with similar absorption features, such as Fe^{3+} Type 1 and Fe^{3+} Type 2 are depicted on the map. The carbonates, phyllosilicates, sulfates, and altered minerals map has 32 classes. Minerals with slightly different mineral compositions but similar spectral features are less easily discriminated; thus, some identified classes consist of several minerals with similar spectra, such as the chlorite or epidote class. When comparisons with reference spectra provided no viable match, a designation of "not classified" was assigned to a pixel.

26B.3 Geologic Setting of the Takhar AOI

The Takhar AOI is in the Takhar Province in northeastern Afghanistan. The contrast-enhanced stretch of the natural-color composite of Landsat Thematic Mapper bands in figure 26B–2 provides a general overview of the Takhar AOI terrain and is useful for understanding the general characteristics and distribution of surficial material including rocks and soil, unconsolidated sediments, vegetation, and hydrologic features.

26B.3.1 Topography

Elevations in the Takhar AOI range between 750 and 3,275 m (fig. 26B–3). The highest areas are in the southeast corner of the Takhar AOI in sharply defined mountain ranges and foothills that are commonly controlled by faults. The low areas include agricultural areas in the northeast part of the AOI around the province capital of Taloqan, which is just north of the AOI boundary. Other population centers include the towns of Farkhar in the east, and Chal and Namakab in the southwest.

26B.3.2 Lithology and Structure

The oldest rocks in the Takhar AOI are Ordovician sandstones and shales and Silurian–Devonian limestones and dolomites exposed at the high elevations in the southern part of the area (fig. 26B–4; Doebrich and others, 2006; Abdullah and Chmyriov, 1977). Triassic and Jurassic sedimentary and volcanic rock units cover most of the mountains and hills in the southeastern portion of the area. Lower elevations in the north are covered by Miocene clays and limestones and Quaternary surficial deposits. Mississippian diorite, granodiorites, and granites intrude along the south edge of the area. Small intrusions of Late Triassic granitic rocks occur in the Namurian stage (Ordovician) and Karachatur horizon strata in the eastern portion of the Takhar AOI.

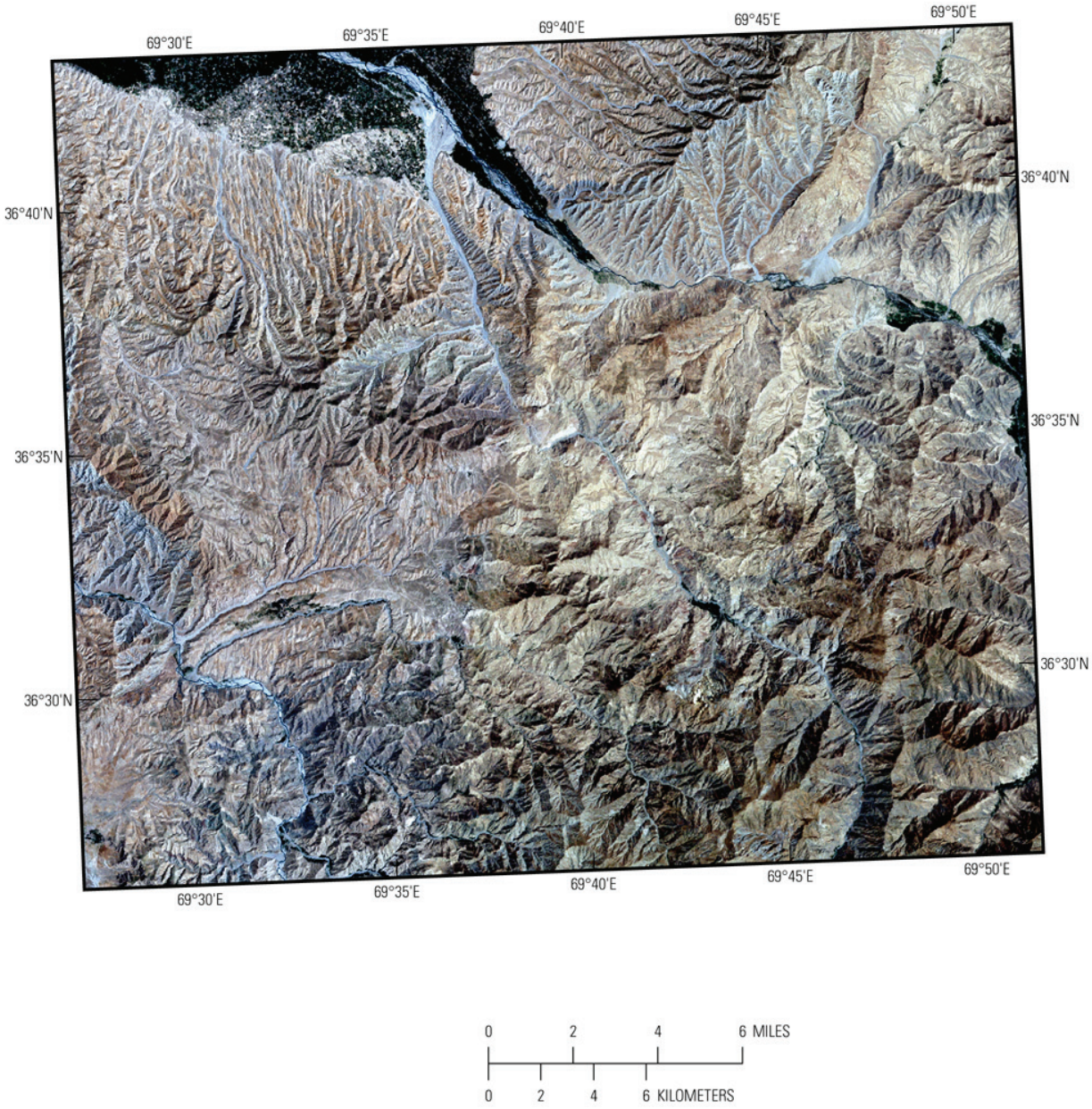

Figure 26B–2. Contrast enhanced Landsat Thematic Mapper natural-color image of the Takhar area of interest.

26B.3.3 Known Mineralization

Figure 26B–5 shows 11 locations where mineralization with a potential for mineral resource development may exist (Peters and others, 2007). A number of different types of industrial mineral deposits, particularly salt deposits, are present within the Takhar AOI. The mineralogical characteristics of the mineralized locations are summarized in table 26B–1. These mineralization occurrences are of two primary types: gypsum and halite. There are also single, small deposits of kaolin and sandstone, and a showing of polymetallic lead-zinc (Pb-Zn).

Table 26B–1. Sites of known mineralization in the Takhar area of interest.

[Data are from Peters and others, 2007).

Name	Deposit type	Major commodity	Deposit size and description
Topcha-Khana	Sedimentary kaolin	China clay	Small, thickness of 4 to 5 m
Sary-Kan	Bedded gypsum	Gypsum	No data
Sary-Kaja	Unknown gypsum	Gypsum	Occurrence, thickness of 150 m
Chal	Bedded gypsum	Gypsum	Occurrence, thickness of several meters
Taqcha Khana	Salt domes	Gypsum, halite	No data
Namakob	Evaporite	Halite	Medium, thickness of 400 m, width of 1,500 m
Nemakab	Unknown halite	Halite	No data
Chal-I	Bedded salt	Halite	Small, extent of 1 km.
Chal-II	Bedded salt	Halite	Small, depth of 20 m
Unnamed	Polymetallic vein	Pb Zn	Showing, thickness of 0.2 m
Farkhar Sandstone	Unknown sandstone	Quartzose sandstones	Small, thickness of 50 to 120 m, extent of 1.2 to 8 km

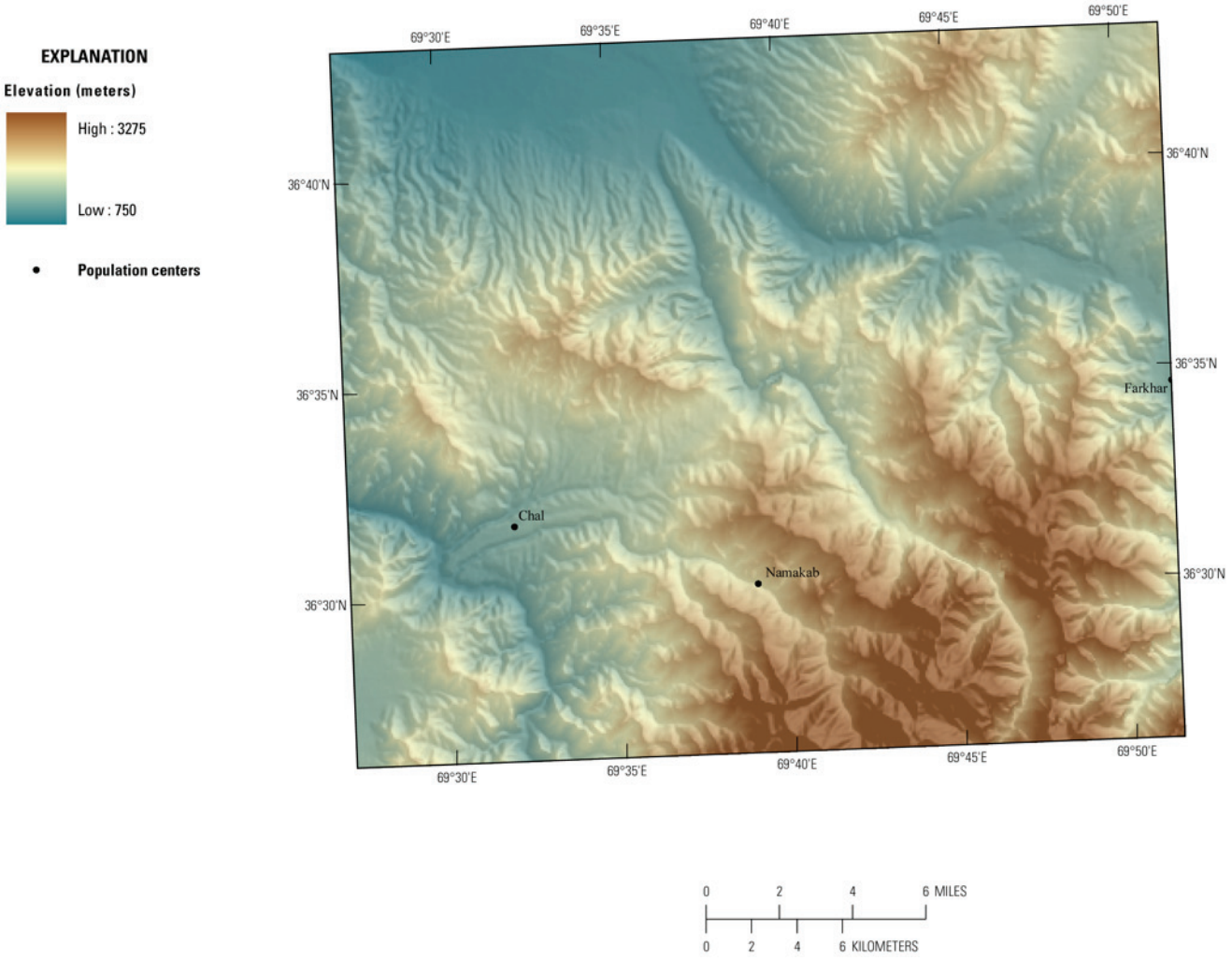

Figure 26B–3. Elevations and topography of the Takhar area of interest.

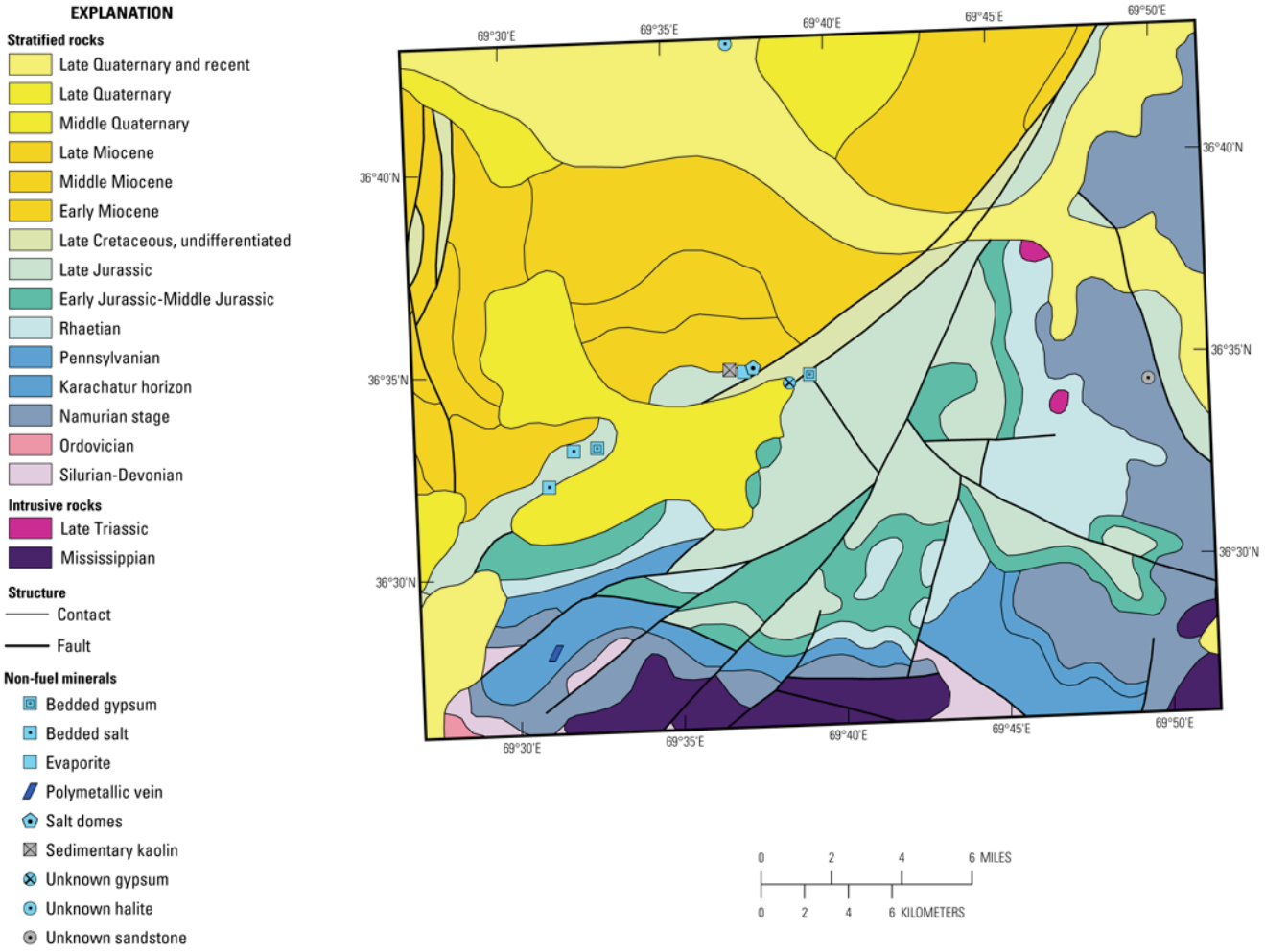

Figure 26B–4. Geologic map of the Takhar area of interest from Doebrich and others (2006) and Abdullah and Chmyriov (1977).

The largest rock-salt deposit of Namakob is in gypsum-salt domes, several kilometers in diameter, formed in a Jurassic sequence overlain by Paleogene–Neogene sedimentary rocks; the domes consist of white and gray, locally reddish, rock salt having a salt content reaching 99 percent by volume (Abdullah and others, 1977). Rock salt occurring in Upper Jurassic rocks has been discovered on the side of the Chal Valley over a distance of 1 km (Chal-I and Chal-II deposits) (Abdullah and others, 1977).

Gypsum (Sary-Kan deposit) has been found alternating with clay in a 150-m-thick unit in Upper Jurassic sedimentary rocks (Abdullah and others, 1977). Gypsum beds (Chal deposit), a few meters thick, lie between Upper Jurassic clay and siltstone (Abdullah and others, 1977).

A kaolin clay bed 4 to 5 m thick occurs between Upper Jurassic conglomerates (at Taqcha Khana). The clay is dark gray to black with brown patches and is thin bedded (Abdullah and others, 1977).

26B.4 Mineral Maps of the Takhar Area of Interest

Analysis of the HyMap imaging spectrometer data of the Takhar AOI using spectroscopic methods resulted in the identification of a wide variety of minerals exposed at the surface. Although the occurrence of certain minerals may suggest that mineralization processes may have once operated in the area, many of the minerals that were identified are also common rock-forming minerals or minerals that can be derived from the weathering of a wide variety of rock types. Consequently, the distribution patterns of the identified minerals and the geologic context in which they occur are extremely important

in understanding the causes of mapped mineral occurrences and evaluating the possible potential for related mineral deposits.

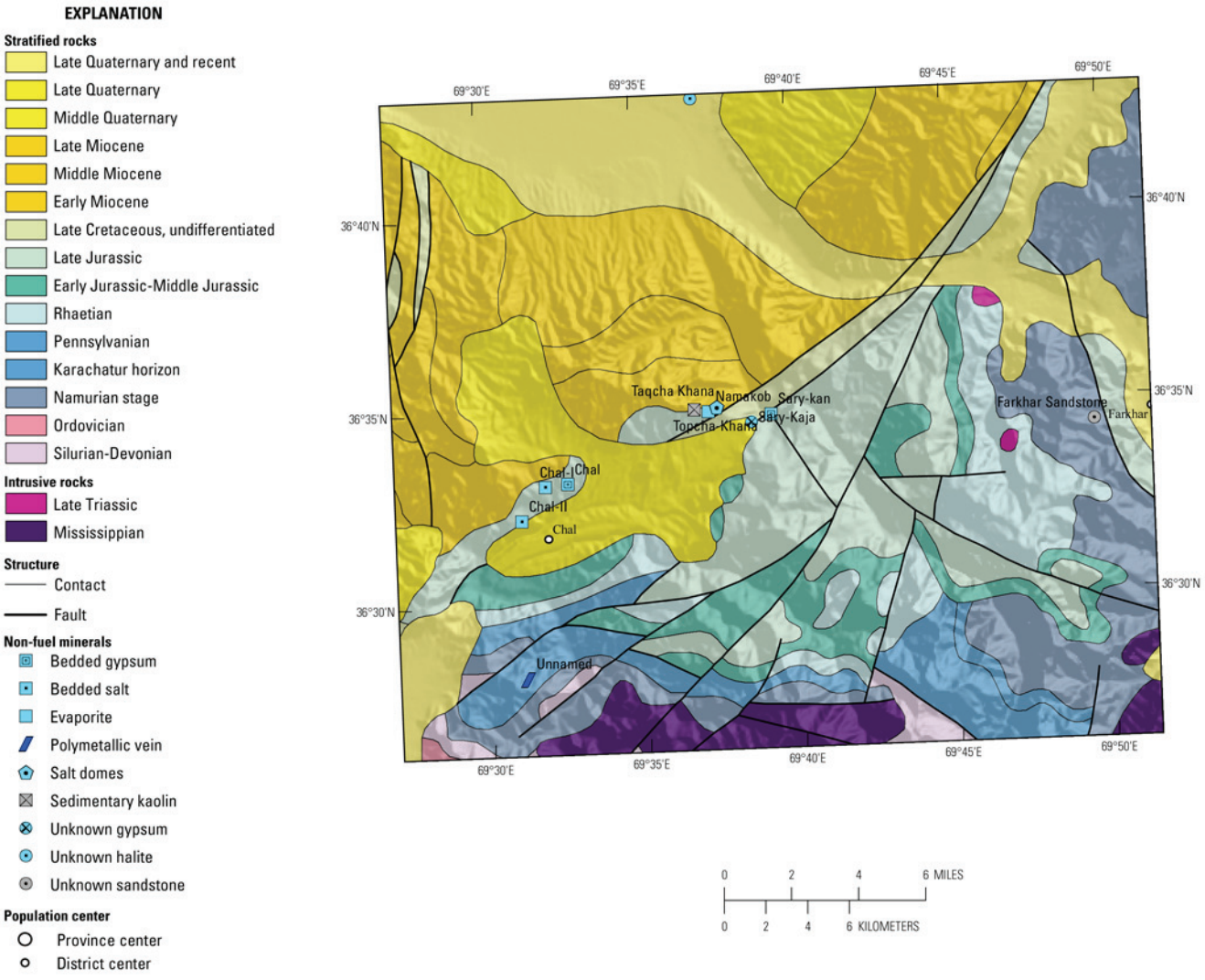

Figure 26B–5. Sites of known mineralization by deposit type (Peters and others, 2007) on the geologic map of the Takhar area of interest (Doebrich and others, 2006; Abdullah and Chmyriov, 1977).

Figure 26B–6 depicts the results of the MICA analyses of the HyMap data for the Takhar AOI for the 2-µm materials including clays, carbonates, phyllosilicates, sulfates, alteration minerals, and other materials. Figure 26B–7 shows the results for the iron-bearing (1 µm) minerals and other materials map. Carbonates cover most of the Takhar AOI. However, muscovites occur over large contiguous areas both within the mapped Mississippian intrusive rocks and in other areas. Distinct patterns of kaolinite clays and gypsum occur in localized patterns, especially in the center of the AOI. Epidote and chlorite were found in spatially consistent patterns near the southern edge of the AOI (see fig. 26B–6).

Because of the large number of classes represented and the subtleties of the distribution patterns represented in these image maps, it is instructive to display these results as a series of image maps each depicting a selected group of minerals that are mineralogically related or commonly occur together in special geologic environments (figs. 26B–8 to 26B–12). Figure 26B–8 shows the distribution of carbonate minerals in the Takhar AOI, whereas figure 26B–9 shows where clay minerals and micas occur. The distribution of iron oxide and hydroxide minerals is displayed in figure 26B–10. Minerals commonly found in hydrothermally altered rocks are mapped in figure 26B–11 and secondary minerals often associated with mineralized and (or) weathered rocks are mapped in figure 26B–12.

26B.4.1 Carbonate Minerals

Carbonate minerals, either calcite or dolomite, were mapped over a large majority of the Takhar AOI (fig. 26B–8). In general, calcite is mapped within every geologic unit. Dolomite mixed with calcite and (or) clay occurs in a less spatially consistent pattern. None of the known mineralized areas are highlighted by the carbonate minerals map, nor do any previously unknown areas of potential mineralization appear to be identified.

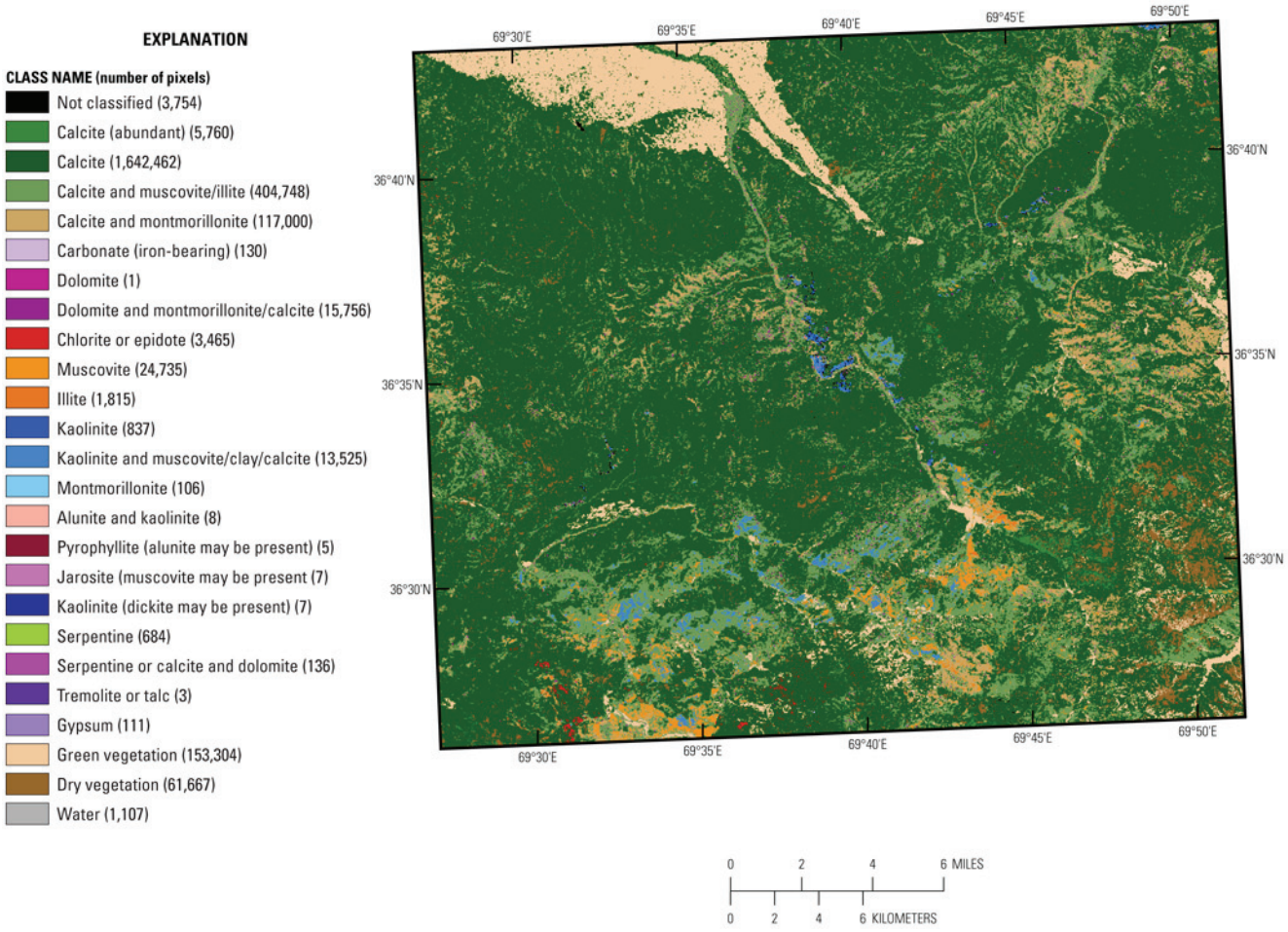

Figure 26B–6. Map of carbonates, phyllosilicates, sulfates, altered minerals, and other materials derived from HyMap data in the Takhar area of interest.

26B.4.2 Clays and Micas

Muscovite concentrations were mapped in the Mississippian intrusive rocks in the southwestern part of the Takhar AOI (fig. 26B–9). In addition, muscovites were detected within and nearby the mapped unit of Late Triassic intrusive rocks. However, muscovites were also found distributed within Rhaetian and Late Jurassic stratified rock units, suggesting that mineral distributions detected with HyMap data could help in the refinement of lithologic contacts. Epidote and chlorite were found primarily in association with Namurian stage and Karachatur horizon sedimentary rocks in the southwest portion of the Takhar AOI. Kaolinites are distributed mostly in Jurassic sedimentary rocks, with additional occurrences of spatially consistent clusters of pixels in Late Cretaceous sedimentary rocks. In the center of the Takhar AOI, kaolinite is found in association with the Sary-Kan bedded gypsum mineral deposit and the Sary-Kaja gypsum mineral occurrence. The Taqcha Khana kaolin deposit is 3 km east of large areas of mapped kaolinite, although the pixels surrounding the indicated

location of that deposit contain a mixture of carbonates and clays; the proximity of the large areas of kaolin suggest the coordinates of the deposit may need adjustment.

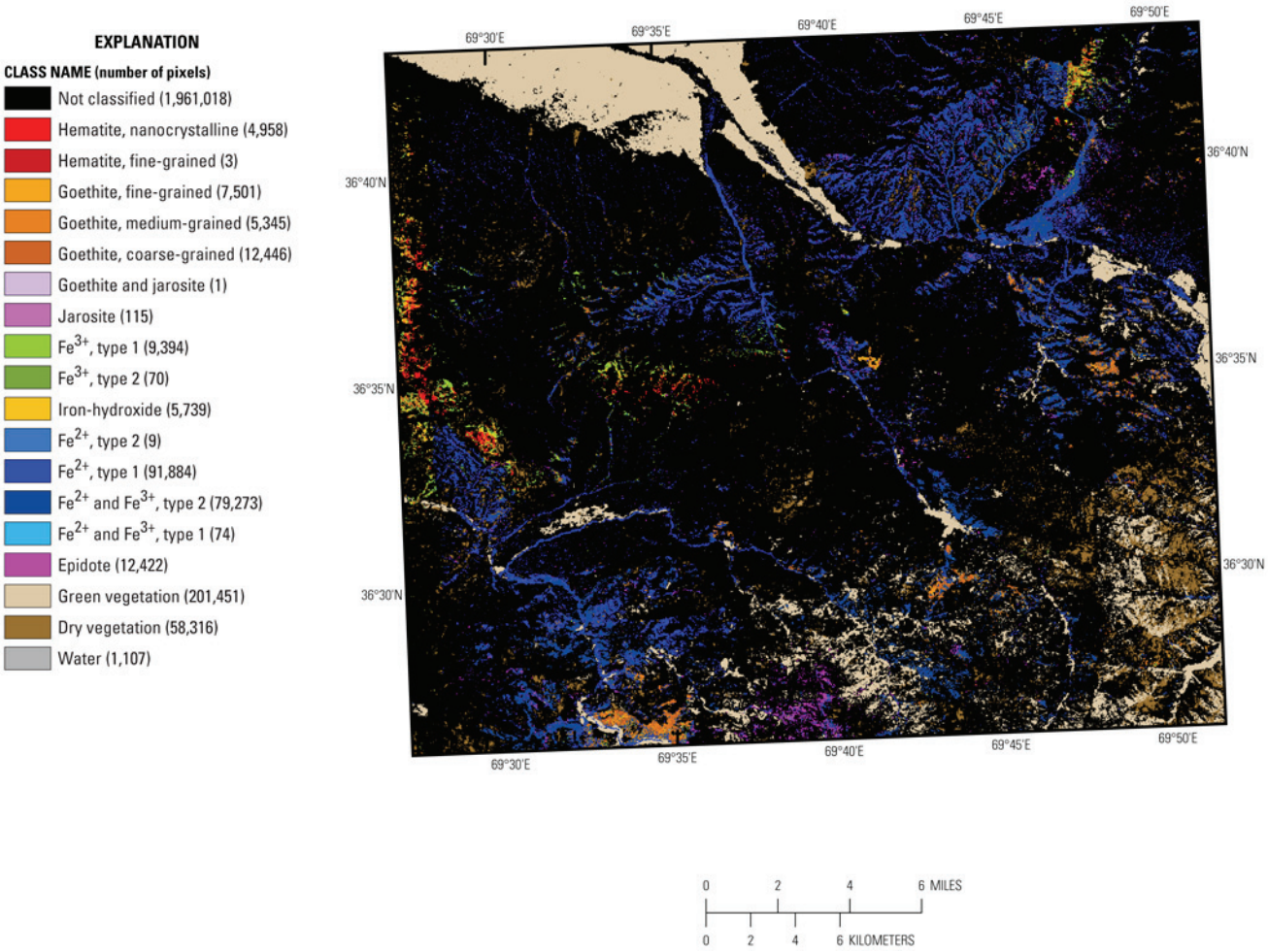

Figure 26B–7. Map of iron-bearing minerals and other materials derived from HyMap data in the Takhar area of interest.

26B.4.3 Iron Oxides and Hydroxides

The Takhar AOI contains conspicuous areas of goethite in the southwest and hematite along the western edge (fig. 26B–10). An area containing both hematite and goethite occurs in the northwestern part of the AOI. More pixels of epidote are found in this map of the AOI, derived from the 1-µm map, in comparison to the epidote or chlorite class in the 2-µm map, due in part to the lack of spectral competitors in the materials of the 1-µm reference spectra.

26B.4.4 Common Alteration Minerals

Most of the minerals in this group are commonly present in hydrothermally altered rocks associated with epithermal mineral deposits (fig. 26B–11). Consequently, where they occur in distinct clusters is of great interest in terms of potential mineral deposits. However, the minerals do not occur in distributions that are suggestive of such alteration in the Takhar AOI. Gypsum is found in the center of the Takhar AOI with kaolinite in the vicinity of the Sary-Kan bedded gypsum mineral deposit and the Sary-Kaja gypsum mineral occurrence.

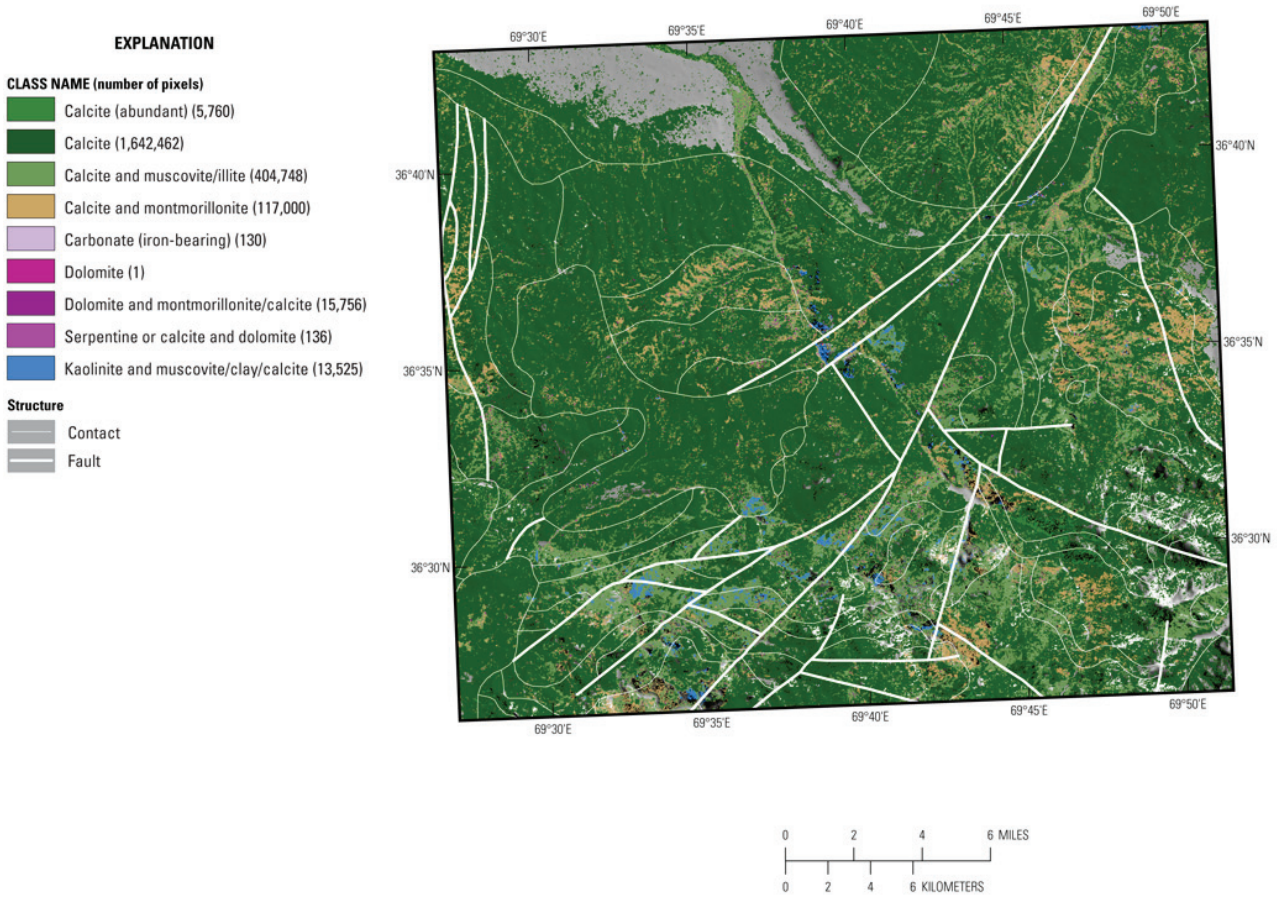

Figure 26B–8. Map of distribution of carbonate minerals derived from HyMap data in the Takhar area of interest.

26B.4.5 Common Secondary Minerals

Secondary minerals in the epidote and chlorite or epidote classes (fig. 26B–12) occur mostly in the southern part of the Takhar AOI. There are, however, several small clusters of the epidote class to the northeast of the Takhar AOI.

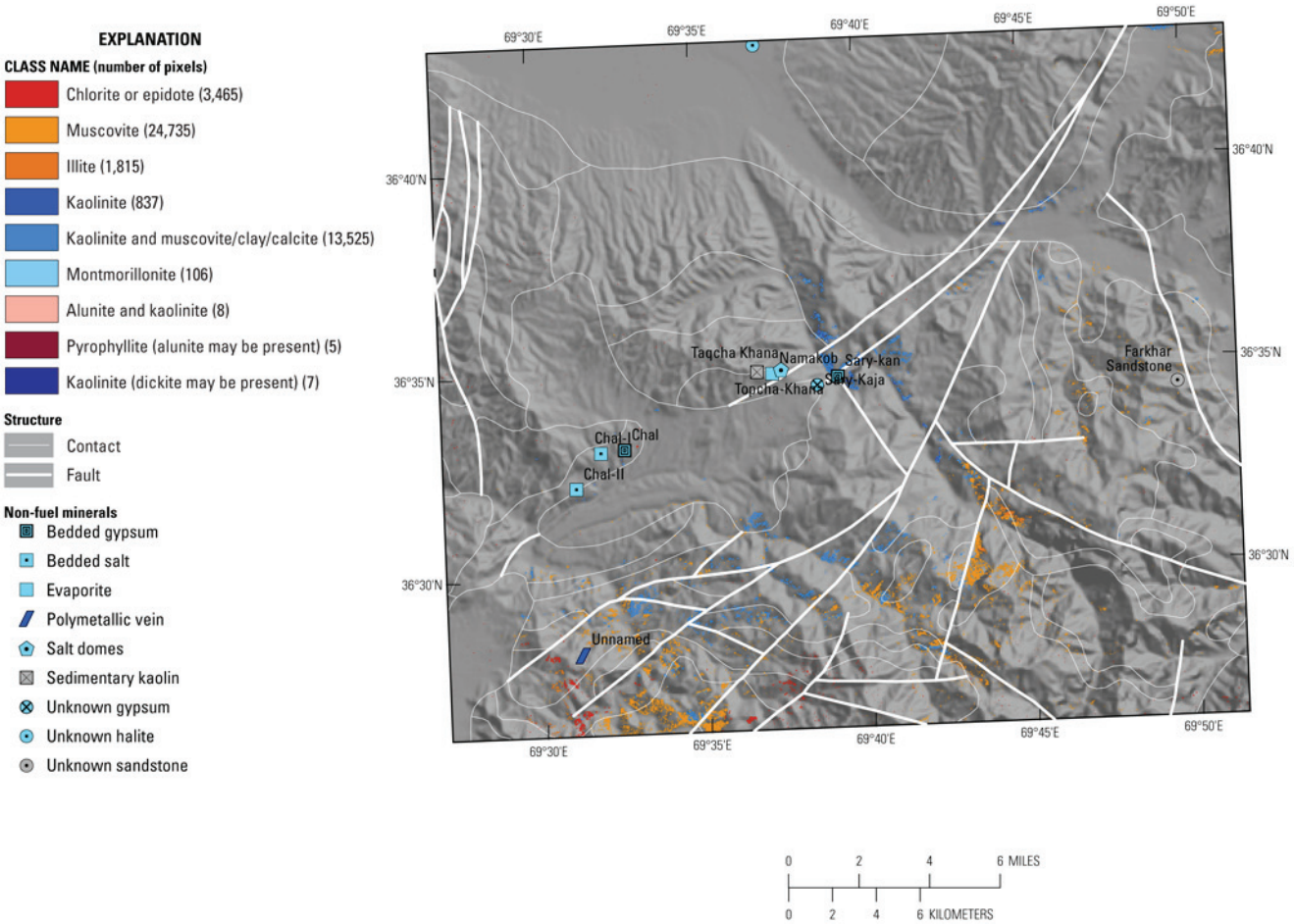

Figure 26B–9. Map of distribution of clay and mica minerals derived from HyMap data in the Takhar area of interest.

26B.4.6 Gypsum and Salt

A MICA analysis using only gypsum in the list of reference spectrum was conducted to expand the mapping of gypsum for greater detail. The result of that mapping is shown in figure 26B–13, in which the gypsum is primarily distributed in the center of the Takhar AOI with concentrations of gypsum stretching to the southwest and northeast spanning the entire area. These previously unknown mineral concentrations will be discussed in more detail in the anomaly map portion of this publication (King, Johnson, and others, 2011). Halite does not have any diagnostic absorption features in the wavelengths covered by the HyMap imaging spectrometer and was not included as a reference spectrum in the MICA analyses. As a result, there is no direct evidence of halite deposits in the imaging spectrometer data. However, the unmapped pixels in the 2-µm map around the areas that mapped as gypsum near the Chal, Chal-I, and Chal-II mineral occurrences (see fig. 26B–14) were examined and found to lack strong absorption features. The lack of absorption features is consistent with the spectral profiles of halite and other evaporite minerals and may be indicative of salt deposits.

26B.4.7 Coal

Direct detection of coal was not attempted using spectral feature analysis of imaging spectrometer data, due to the lack of diagnostic absorption features in coal. A comparison of the 2-µm map of materials, which includes clays, carbonates, phyllosilicates, sulfates, and altered minerals, to

known occurrences of coal (Abdullah and others, 1977) and the Lower to Middle Jurassic geologic unit associated with coal is shown in figure 26B–15. The known coal deposits appear to be associated with areas of kaolinite, kaolinite mixed with muscovite/clay/calcite, and calcite mixed with muscovite/illite. Given this indication, further study of these associations and refinement of HyMap analysis using spectral measurements of field samples of surface materials common to the known coal resources is warranted.

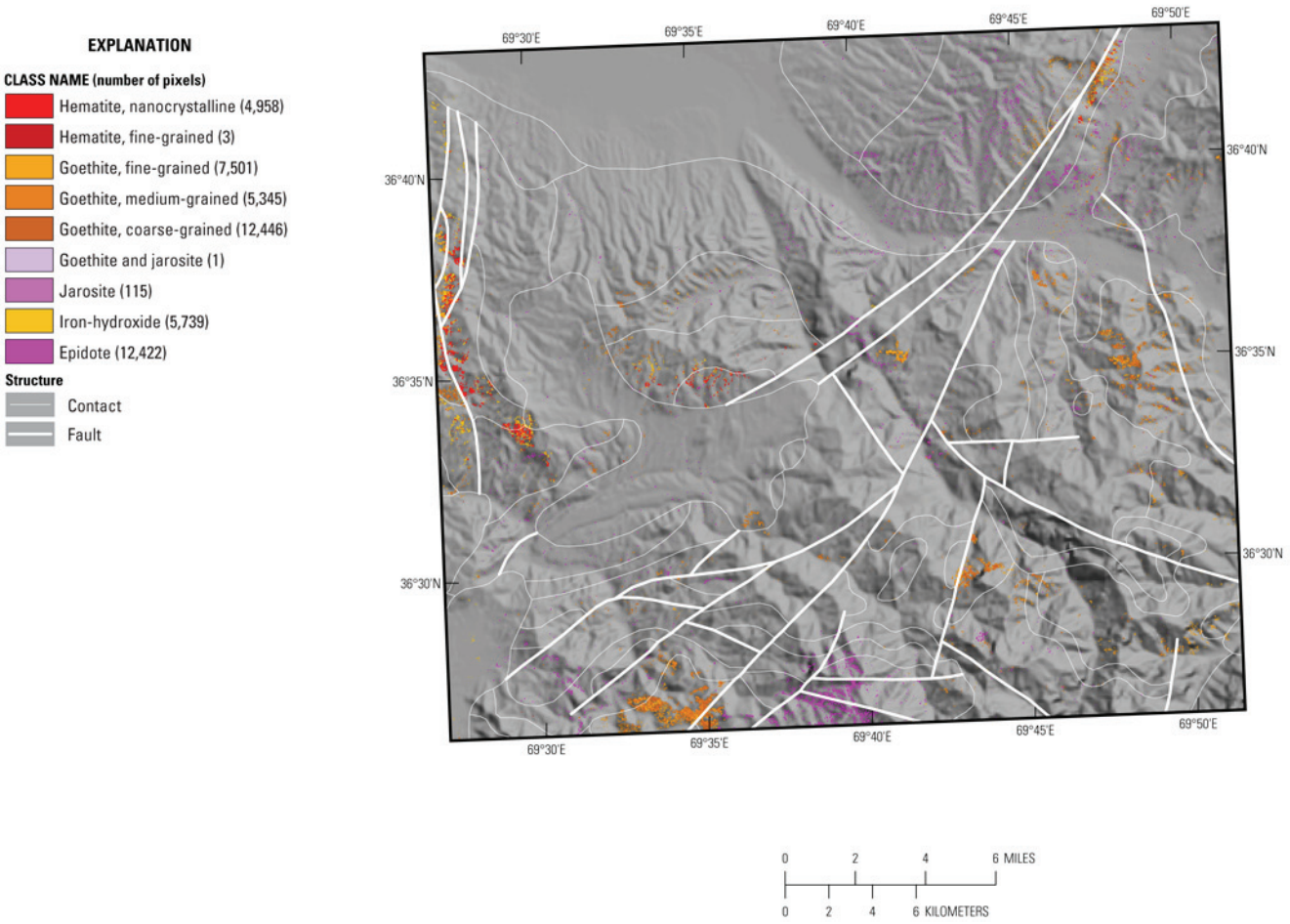

Figure 26B–10. Map of distribution of iron oxide and hydroxide derived from HyMap data in the Takhar area of interest.

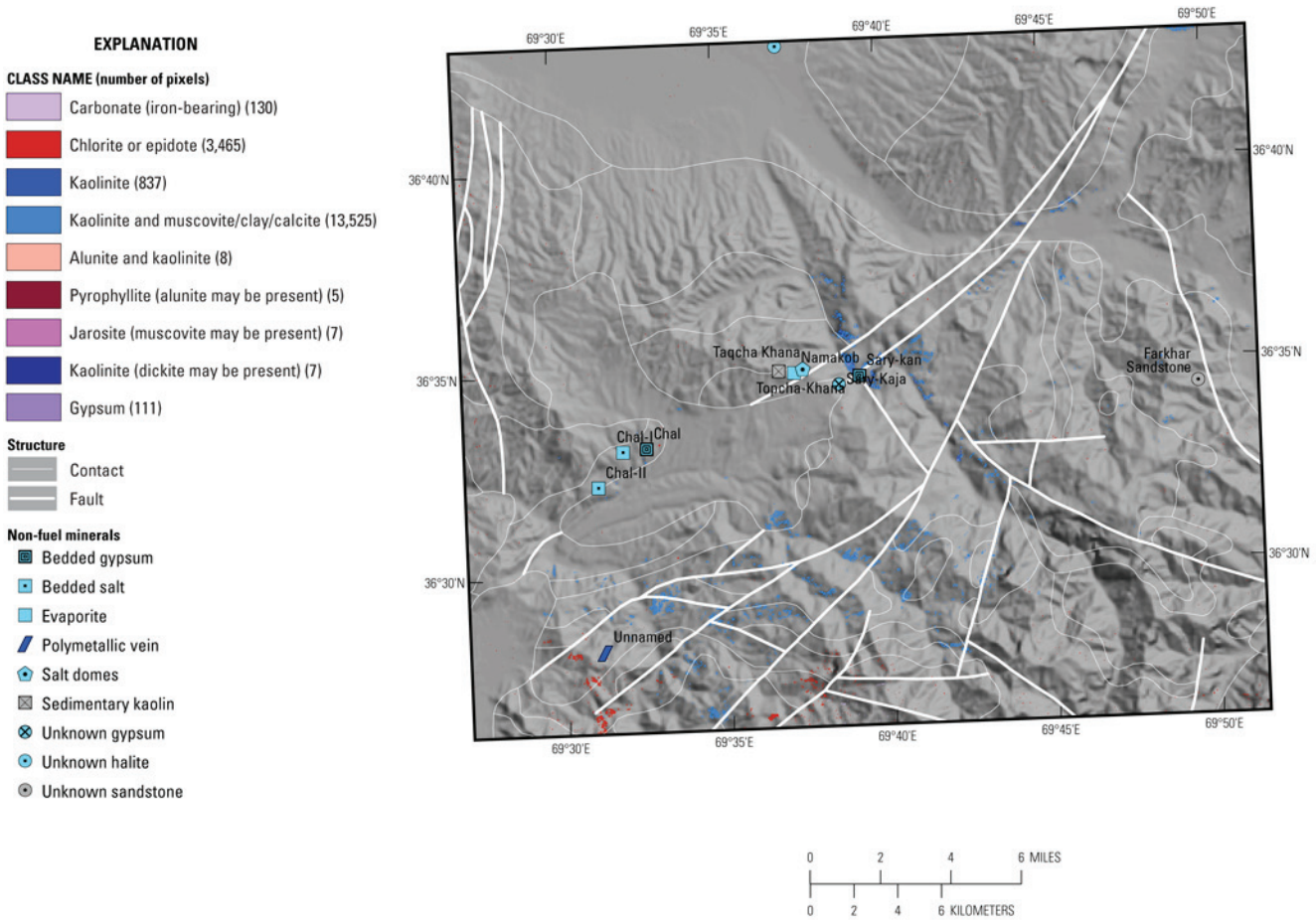

Figure 26B–11. Map of distribution of common alteration minerals derived from HyMap data in the Takhar area of interest.

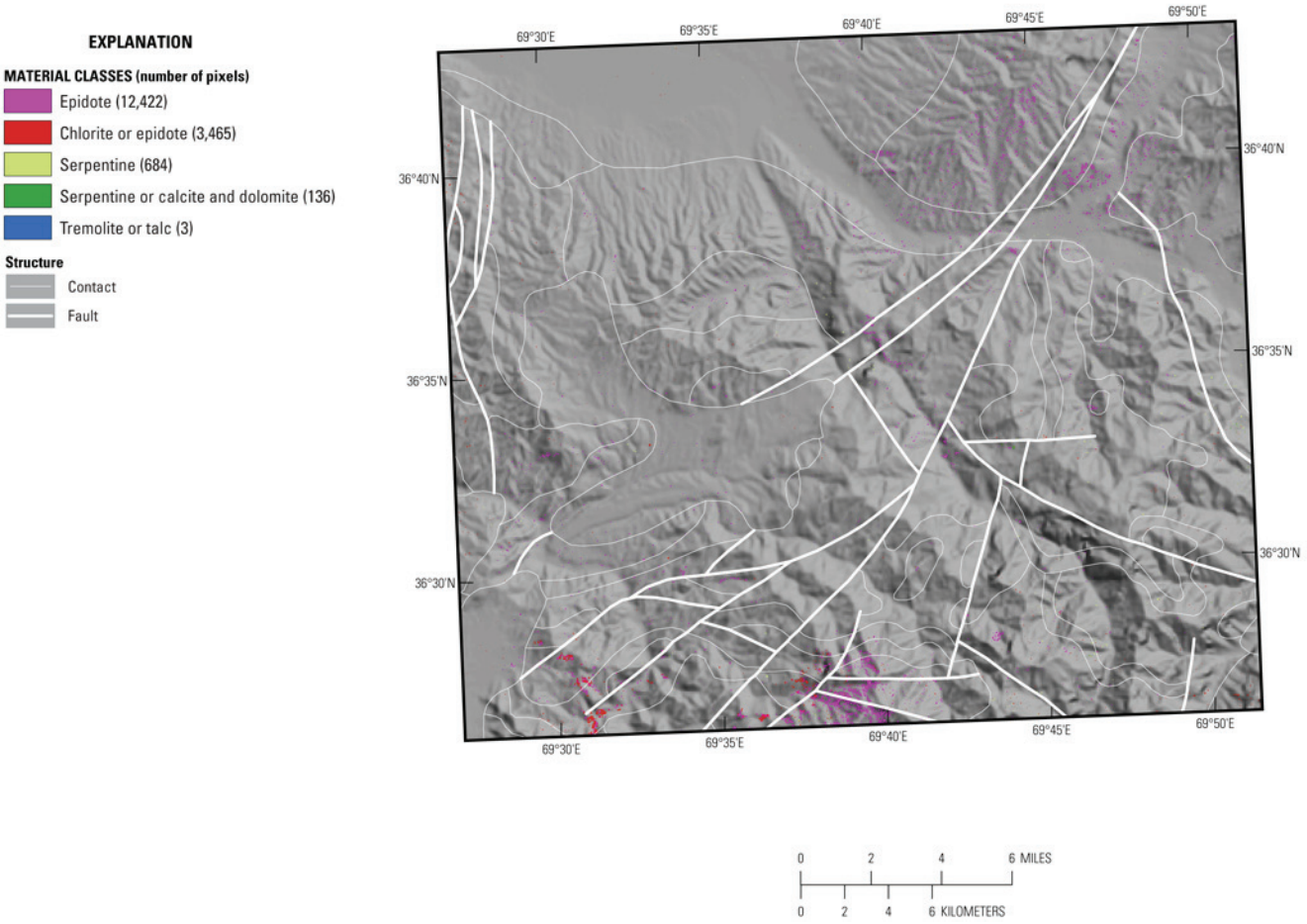

Figure 26B–12. Map of distribution of common secondary minerals derived from HyMap data in the Takhar area of interest.

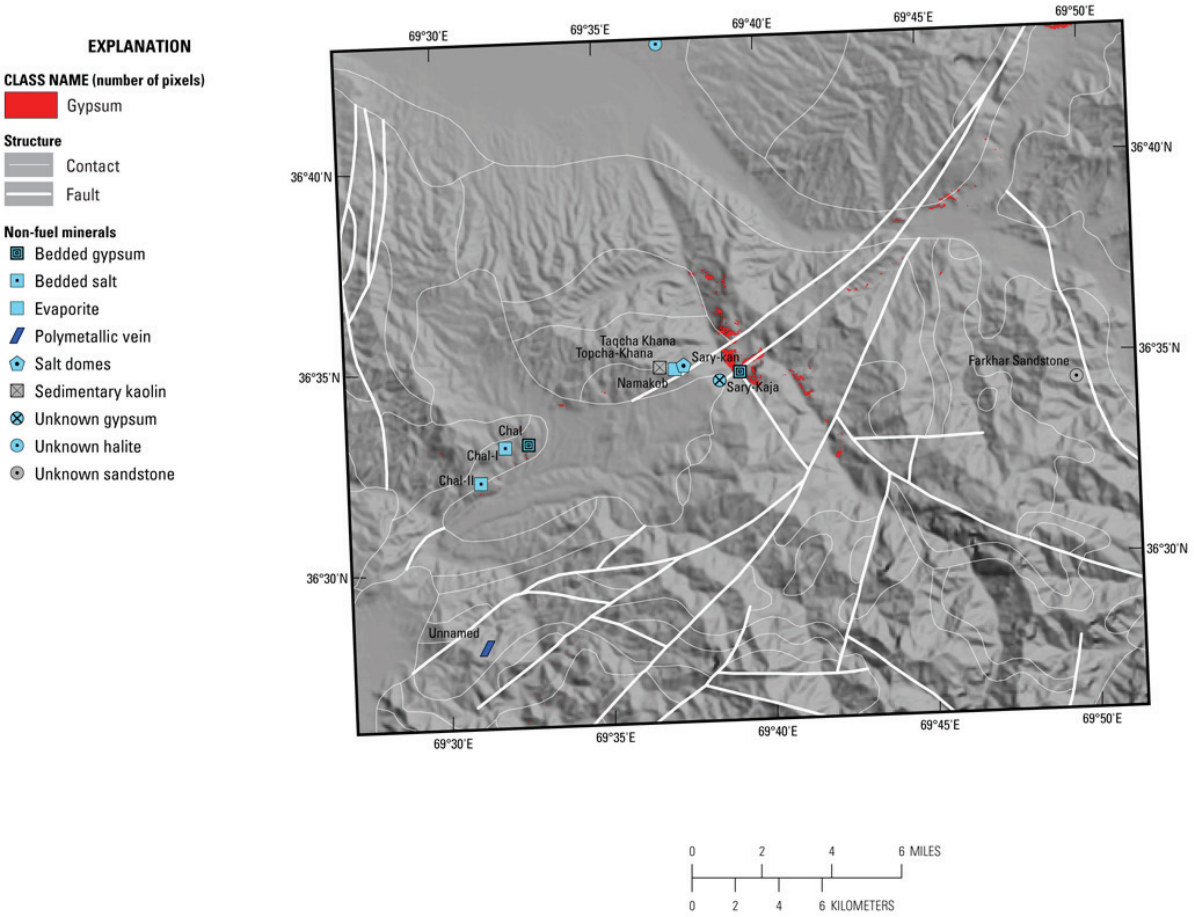

Figure 26B–13. Map of gypsum distribution derived from HyMap data in the Takhar area of interest.

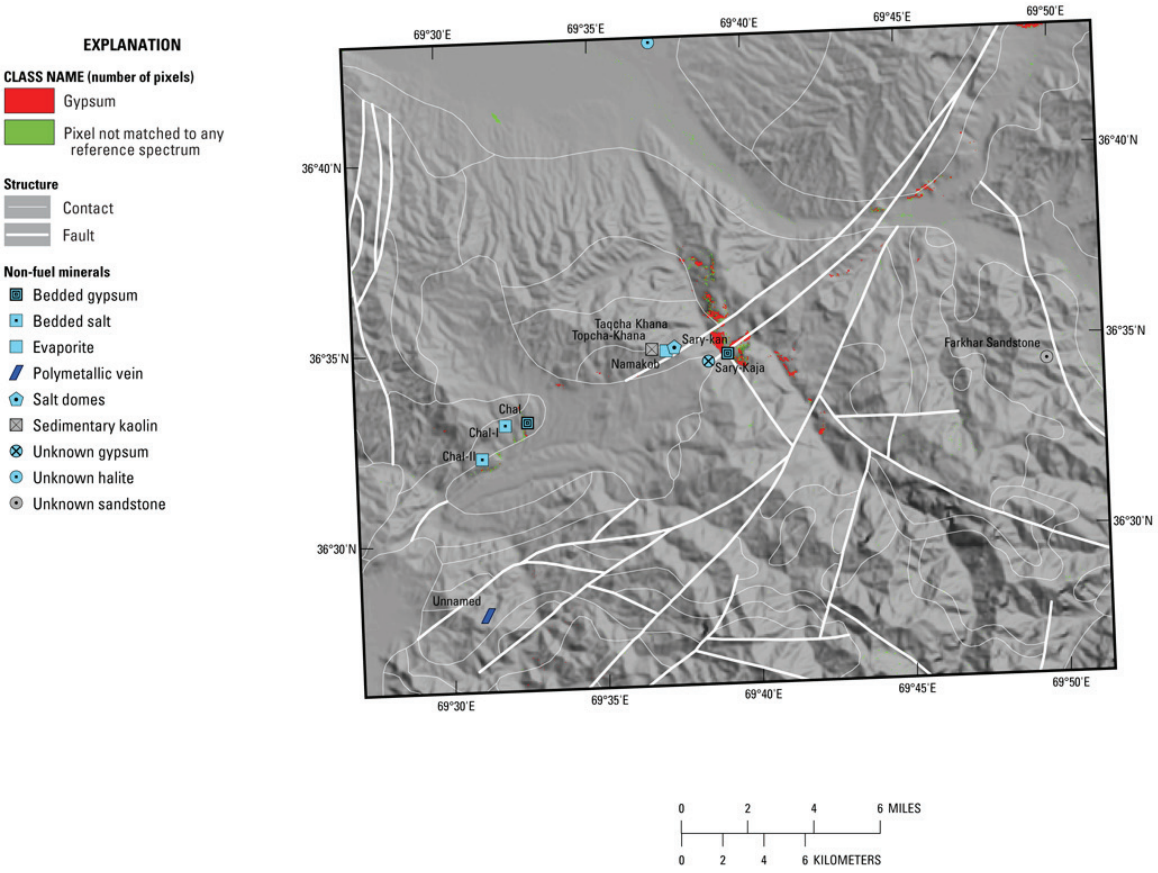

Figure 26B–14. Map of the distributions of gypsum and unmapped pixels derived from HyMap data for the region around known gypsum and salt deposits in the Takhar area of interest.

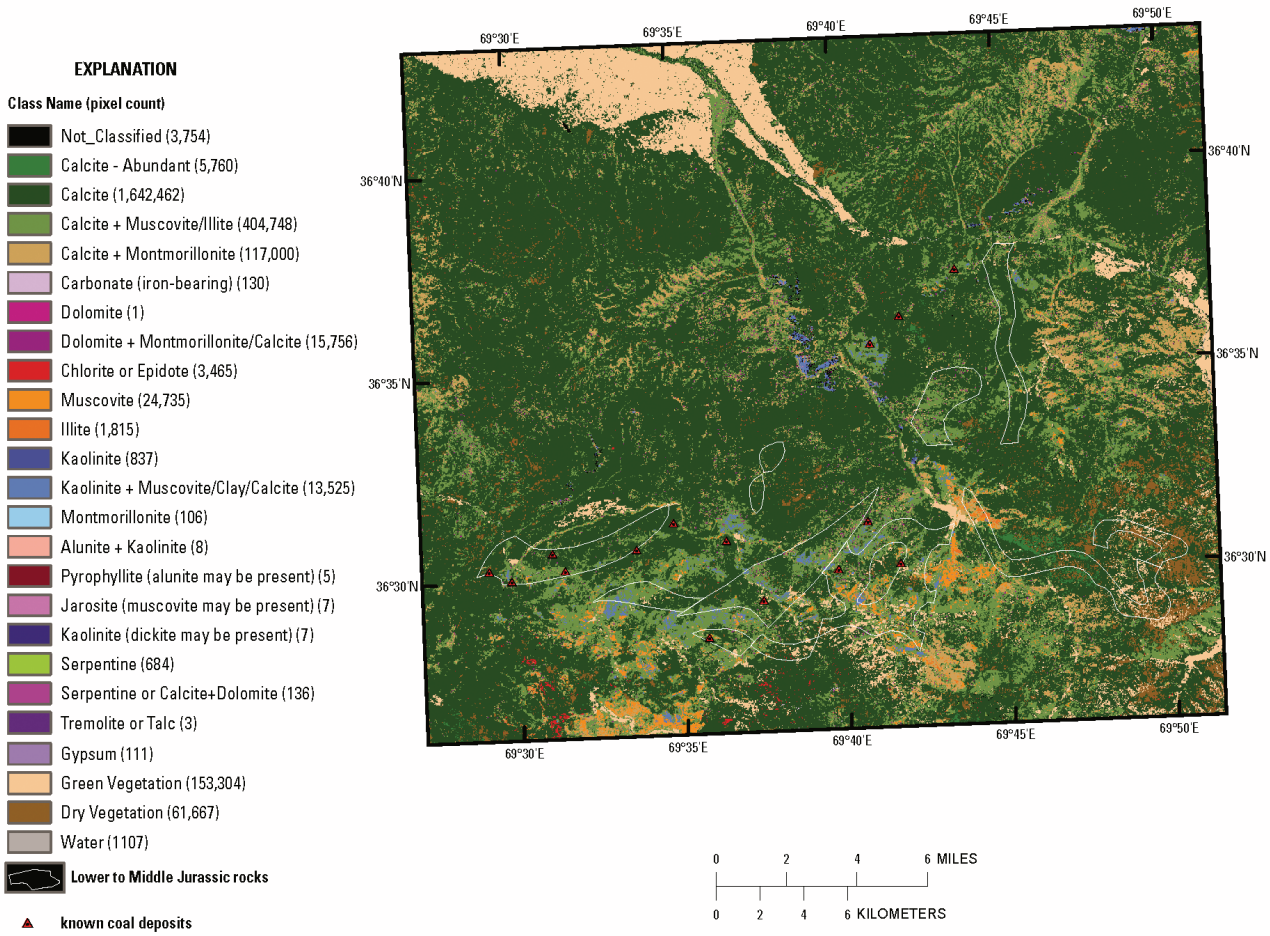

Figure 26B–15. Map of carbonates, phyllosilicates, sulfates, altered minerals, and other materials derived from HyMap data in relation to known coal occurrences (Abdullah and others, 1977) in the Takhar area of interest.

26B.5 Summary

Carbonates cover most of the Takhar AOI. Muscovites were mapped in greatest concentration in the Mississippian intrusive rocks in the southwestern part of the Takhar AOI and within and nearby the mapped Late Triassic intrusive rocks. Muscovites are also found distributed within Rhaetian and other Late Jurassic stratified rocks, suggesting that mineral distributions detected with HyMap data could help in the refinement of lithologic contacts. Epidote and chlorite were found in spatially consistent patterns near the southern edge of the AOI in association with Namurian stage and Karachatur horizon stratified rock units. Distinct patterns of kaolinite clays and gypsum occur in localized patterns, especially in the center of the AOI. Kaolinites are distributed mostly in Jurassic sedimentary rocks, with additional occurrences of spatially consistent groups of pixels in Late Cretaceous units. In the center of the Takhar AOI, kaolinite is found in association with the Sary-Kan bedded gypsum mineral deposit and the Sary-Kaja gypsum mineral occurrence. The spectral signature of gypsum was detected in the HyMap data, primarily distributed in the center of the Takhar AOI, adjacent to the bedded gypsum deposit at Sary-Kan and the gypsum occurrence at Chal, with concentrations of gypsum stretching to the southwest and northeast spanning the entire AOI. Although halite does not have any strong diagnostic absorption features in the wavelengths covered by the HyMap imaging spectrometer, an examination of unmapped pixels in the 2-µm map revealed spectra that lack strong absorption features, possibly consistent with halite and other evaporite minerals. These pixels, which did not match any reference spectra, are distributed along the same trend as Chal-I and Chal-II salt deposits and the pixels in which gypsum was detected. Within and around rocks of Lower to Middle Jurassic age, the known coal deposits appear to

be associated with pixels in which kaolinite mixed with other materials was mapped in the HyMap data. Given this indication, more detailed analysis of HyMap data around these coal occurrences may help establish the distribution of this resource.

26B.6 References Cited

Abdullah, Sh., and Chmyriov, V.M., 1977, Geological map of Afghanistan: Kabul, Afghanistan, Ministry of Mining and Industry of Democratic Republic of Afghanistan, scale 1:500,000.

Abdullah, Sh., Chmyriov, V.M., Stazhilo-Alekseev, K.F., Dronov, V.I., Gannan, P.J., Rossovskiy, L.N., Kafarskiy, A.Kh., and Malyarov, E.P., 1977, Mineral resources of Afghanistan (2d ed.): Kabul, Afghanistan, Republic of Afghanistan Geological and Mineral Survey, 419 p.

Cocks, T., Jenssen, R., Stewart, A., Wilson, I., and Shields, T., 1998, The HyMap airborne hyperspectral sensor—The system, calibration and performance, *in* Schaepman, M., Schlapfer, D., and Itten, K.I., eds., Proceedings of the 1st EARSeL Workshop on Imaging Spectroscopy, 6–8 October 1998, Zurich: Paris, European Association of Remote Sensing Laboratories, p. 37–43.

Davis, P.A., 2007, Landsat ETM+ false-color image mosaics of Afghanistan: U.S. Geological Survey Open-File Report 2007–1029, 22 p. (Also available at *http://pubs.usgs.gov/of/2007/1029/*.)

Doebrich, J.L., and Wahl, R.R., comps., *with contributions by* Doebrich, J.L., Wahl, R.R., Ludington, S.D., Chirico, P.G., Wandrey, C.J., Bohannon, R.G., Orris, G.J., Bliss, J.D., and ____, 2006, Geologic and mineral resource map of Afghanistan: U.S. Geological Survey Open File Report 2006–1038, scale 1:850,000, available at *http://pubs.usgs.gov/of/2006/1038/*.

Hoefen, T.M., Kokaly, R.F., and King, T.V.V., 2010, Calibration of HyMap data covering the country of Afghanistan, *in* Proceedings of the 15th Australasian Remote Sensing and Photogrammetry Conference, Alice Springs, Australia, September 12–17, 2010, p. 409, available at *http://dl.dropbox.com/u/81114/15ARSPC-Proceedings.zip/*.

King, T.V.V., Johnson, M.R., Hoefen, T.M., Kokaly, R.F., and Livo, K.E., 2011, Mapping potential mineral resource anomalies using HyMap data, *in* King, T.V.V., Johnson, M.R., Hubbard, B.E., and Drenth, B.J., eds, Identification of mineral resources in Afghanistan—Detecting and mapping resource anomalies in prioritized areas using geophysical and remote sensing (ASTER and HyMap) data in Afghanistan: U.S. Geological Survey Open-File Report 2011–1229, available at *http://pubs.usgs.gov/of/2011/1229/*.

King, T.V.V., Kokaly, R.F., Hoefen, T.M., and Knepper, D.H., 2010, Resource mapping in Afghanistan using HyMap data, *in* Proceedings of the 15th Australasian Remote Sensing and Photogrammetry Conference, Alice Springs, Australia, September 12–17, 2010, p. 500, available at *http://dl.dropbox.com/u/81114/15ARSPC-Proceedings.zip/*.

King, T.V.V., Kokaly, R.F., Hoefen, T.M., Dudek, K. and Livo, K.E., 2011, Surface materials map of Afghanistan—Iron-bearing minerals and other materials: U.S. Geological Survey Scientific Investigations Map 3152–B.

Kokaly, R.F., King, T.V.V., and Livo, K.E., 2008, Airborne hyperspectral survey of Afghanistan 2007—Flight line planning and HyMap data collection: U.S. Geological Survey Open-File Report 2008–1235, 14 p.

Kokaly, Ray, 2011, PRISM—Processing routines in IDL for spectroscopic measurements: U.S. Geological Survey Open-File Report 2011–1155, available at *http://pubs.usgs.gov/of/2011/1155/*.

Kokaly, R.F., King, T.V.V., Hoefen, T.M., Dudek, K. and Livo, K.E., 2011, Surface materials map of Afghanistan—Carbonates, phyllosilicates, sulfates, altered minerals, and other materials: U.S. Geological Survey Scientific Investigations Map 3152–A.

Peters, S.G., Ludington, S.D., Orris, G.J., Sutphin, D.M., Bliss, J.D., and Rytuba, J.J., eds., and the U.S. Geological Survey-Afghanistan Ministry of Mines Joint Mineral Resource Assessment Team, 2007, Preliminary non-fuel mineral resource assessment of Afghanistan: U.S. Geological Survey Open-File Report 2007–1214, 810 p., 1 CD–ROM. (Also available at *http://pubs.usgs.gov/of/2007/1214/*.)